Liquid Crystals
Publication details, including instructions for authors and subscription information:
http://www.informaworld.com/smpp/title~content=t713926090

Lamellar-non-lamellar phase transitions in synthetic glycoglycerolipids studied by time-resolved X-ray diffraction

Rumiana Tenchova[a]; Boris Tenchov[a]; Hans-JÜRgen Hinz[b]; Peter J. Quinn[c]
[a] Institute of Biophysics, Bulgarian Academy of Sciences, Sofia, Bulgaria [b] Institut für Physikalische Chemie, Westfälische Wilhelms-Universität, Münster, Germany [c] Division of Life Sciences, King's College London, London, UK

To cite this Article Tenchova, Rumiana , Tenchov, Boris , Hinz, Hans-JÜRgen and Quinn, Peter J.(1996) 'Lamellar-non-lamellar phase transitions in synthetic glycoglycerolipids studied by time-resolved X-ray diffraction', Liquid Crystals, 20: 4, 469 — 482
To link to this Article: DOI: 10.1080/02678299608032061
URL: http://dx.doi.org/10.1080/02678299608032061

LIQUID CRYSTALS, 1996, VOL. 20, NO. 4, 469-482

Lamellar–non-lamellar phase transitions in synthetic glycoglycerolipids studied by time-resolved X-ray diffraction

by RUMIANA TENCHOVA, BORIS TENCHOV
Institute of Biophysics, Bulgarian Academy of Sciences, 1113 Sofia, Bulgaria

HANS-JÜRGEN HINZ
Institut für Physikalische Chemie, Westfälische Wilhelms-Universität, 4400 Münster, Germany

and PETER J. QUINN*
Division of Life Sciences, King's College London, Campden Hill, London W8 7AH, UK

(*Received 17 July 1995; in final form 7 November 1995; accepted 30 November 1995*)

The phase sequences of eight fully hydrated synthetic, stereochemically pure glycoglycerolipids with saturated alkyl chains 12–18 carbon atoms long and a glucose, galactose or mannose head group are followed in real time during heating and cooling scans using synchrotron X-ray diffraction. One of them, 1,2-di-*O*-hexadecyl-3-*O*-β-D-glucosyl-*sn*-glycerol, has been characterized by X-ray diffraction for the first time. A summary of the lamellar–non-lamellar transition sequences and reversibility for all eight glycoglycerolipids studied is provided. It includes also observations of intermediate phases, previously not detected. Lattice parameters of the various phases have been determined as functions of chain length in monoglucosides. While the repeat periods of the lamellar phases increase linearly with chain length, an anomalously high lattice spacing of the inverted hexagonal phase is observed at a chain length of 14 carbon atoms. This maximum coincides with the disappearance of the cubic phases from the phase sequence upon chain elongation from 12 to 14 carbon atoms. It thus appears that the expanded H_{II} phase in 14-Glc retains structural characteristics of the anticipated cubic phases. Upon heating to high temperatures, its high lattice spacing gradually approaches that of the 'normal' hexagonal phase. A direct transition from lamellar subgel to inverted hexagonal phase has been observed to proceed without intermediate structures, but with an extended phase coexistence region, in 1,2-di-*O*-tetradecyl-3-*O*-β-D-galactosyl-*sn*-glycerol and 1,2-di-*O*-octadecyl-3-*O*-β-D-galactosyl-*sn*-glycerol. This transition is not reversible on cooling when lamellar phases skipped in the heating scan intervene. By contrast, the direct lamellar gel-inverted hexagonal phase transitions are fully reversible with minor or absent temperature hysteresis.

1. Introduction

The glycoglycerolipids are one of the major glycolipid classes, present in plant and animal tissues and in a variety of micro-organisms [1, 2]. Their polymorphic behaviour is less well studied in comparison to phospholipids due in part to the great diversity in their carbohydrate composition [3]. Recently developed synthesis procedures for producing stereochemically pure glycoglycerolipids of defined fatty acid chain composition [4–6] have stimulated the interest in the phase behaviour of this lipid class. As a result of a sizeable body of studies [4, 6–30], considerable progress has been made in the structural and thermodynamic characterization of the glycolipid/water systems. As reported in the cited studies, the glycerolipids with monosaccharide head groups form an impressive variety of lamellar and non-lamellar phases of different stability and display phase sequences strongly dependent on both small differences in the molecular geometry and the temperature prehistory (for a review, see [3]). Introduction of a second or third monosaccharide moiety in the head group region strongly simplifies the phase behaviour of these lipids and suppresses their ability to form non-lamellar structures [4, 10, 15, 23].

In the present work, we studied the phase sequences in eight synthetic, stereochemically pure glycoglycerolipids with saturated ether-linked alkyl chains and glucose (12-Glc, 14-Glc, 16-Glc, 18-Glc), galactose (14-Gal, 14-2,3-

* Author for correspondence.

0267-8292/96 $12·00

Gal, 18-Gal), or mannose (16-Man) monosaccharide head groups (figure 1). All these glycolipids form non-lamellar liquid crystalline phases at high temperatures. We applied synchrotron X-ray diffraction in order to follow in real time the detailed transition pathways between lamellar and non-lamellar phases and to identify possible intermediate structures in heating and cooling phase sequences. This approach revealed specific differences between the direct subgel-inverted hexagonal and gel-inverted hexagonal phase transitions. It demonstrated also the existence of an unusually high lattice spacing of the inverted hexagonal phase at a chain length of 14 carbon atoms in homologous series of dialkylmonoglucosides. An overview of the phase transition sequences and reversibility based on these data for all eight glycoglycerolipids is provided. It describes also intermediate phases which have not been detected in previous studies.

2. Materials and methods

1,2-*O*-dialkyl-3-*O*-β-D-glycosyl-*sn*-glycerols with glucose (Glc), galactose (Gal) or mannose (Man) sugar moieties and saturated alkyl chains 12, 14, 16, or 18 carbon atoms long (12-Glc, 14-Glc, 16-Glc, and 18-Glc; 14-Gal and 18-Gal; 16-Man) and 2,3-di-*O*-tetradecyl-1-*O*-β-D-galactosyl-*sn*-glycerol (14-2, 3-Gal) (figure 1) were synthesized using procedures described elsewhere [5, 8]. The chromatographic purity of all compounds and intermediate products was assured by thin-layer chromatography on silica-gel plates (Merck), and the stereochemical purity was checked by 250 MHz ^{1}H and ^{13}C NMR as previously described [7].

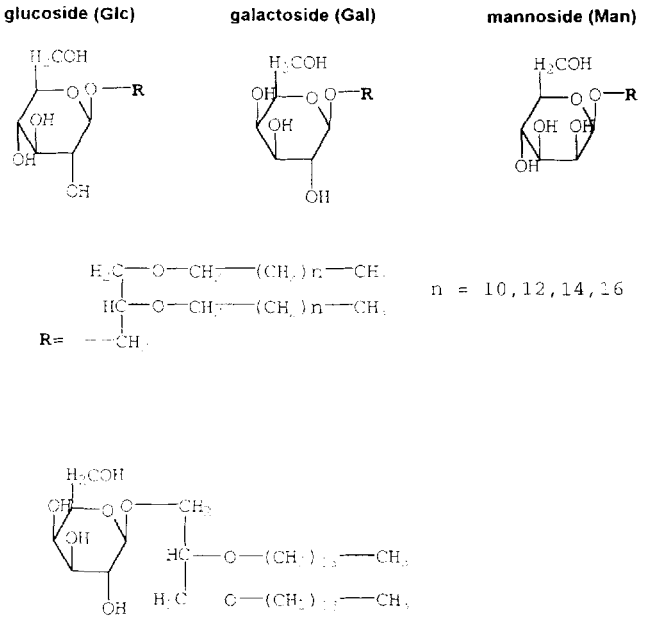

Figure 1. Structural formulae of the sugar head groups of the glycoglycerolipids examined in this study and the 1,2-dialkyl-*sn*-glycerol backbone; the structural formula of 14-2,3-Gal is shown separately.

Time-resolved X-ray measurements were performed on 20 wt % lipid suspensions in quartz-bidistilled water. The lipids were initially hydrated at 20°C for 48 h and dispersed by vortex mixing for 8–10 min at the same temperature. Such sample preparation, without heating above the temperature of the gel–liquid crystalline phase transition of the lipid dispersion, is referred to as 'low-temperature sample preparation' further in the text. Following the first heating, 3–5 heating–cooling cycles were performed.

Time-resolved X-ray diffraction measurements were undertaken using a monochromatic (0·15 nm) focused X-ray beam at stations 7·2 and 8·2 of the Daresbury Synchrotron Radiation Laboratory (UK) as previously described [31]. A Keele flat plate camera with a 512-channel linear detector constructed at the Daresbury Laboratory was used for recording diffraction patterns simultaneously in the low and wide angle ranges. The channel-to-channel resolution was 0·2–0·3 nm for spacings in the range 6–7 nm. The samples were sandwiched between thin mica sheets, 1 mm apart, and were mounted on a modified cryostage (Linkam Scientific Instruments Ltd., Tadworth, UK). Successive cooling and heating scans were performed in defined temperature ranges with scan rates of 2°C min^{-1} and 5°C min^{-1}. X-ray scattering data were acquired in 255 consecutive time frames of 2–8·5 s separated by 50 μs waiting time between the data acquisition frames. Data were stored in a VAX 11/785 computer (Maynard, MA), and analysed using an OTOKO software (EMBL, Hamburg, Germany) program [32]. Scattering intensities were corrected for detector response recorded from a ^{59}Fe source, and spatial calibrations were obtained using Teflon (0·48 nm) as a calibration standard [33]. Under the conditions used to record the dynamic X-ray data, no apparent radiation damage was evident either from the phase behaviour of the samples or by detection of lipid breakdown products in thin-layer chromatograms of the lipid performed upon completion of the diffraction experiments.

3. Results

3.1. *12-Glc*

1st heating $L_c \xrightarrow{40^\circ C} L_\alpha \xrightarrow{55^\circ C} Q^{229} \xrightarrow{58^\circ C} Q^{229} + Q^{224} \xrightarrow{61^\circ C} Q^{224} \xrightarrow{74^\circ C} Q^{224} + H_{II}$

cooling $Q^{224} + H_{II} \xrightarrow{78^\circ C} Q^{224} \xrightarrow{73^\circ C} Q^{229} + Q^{224} \xrightarrow{60^\circ C} Q^{224} + L_\alpha \xrightarrow{48^\circ C}$

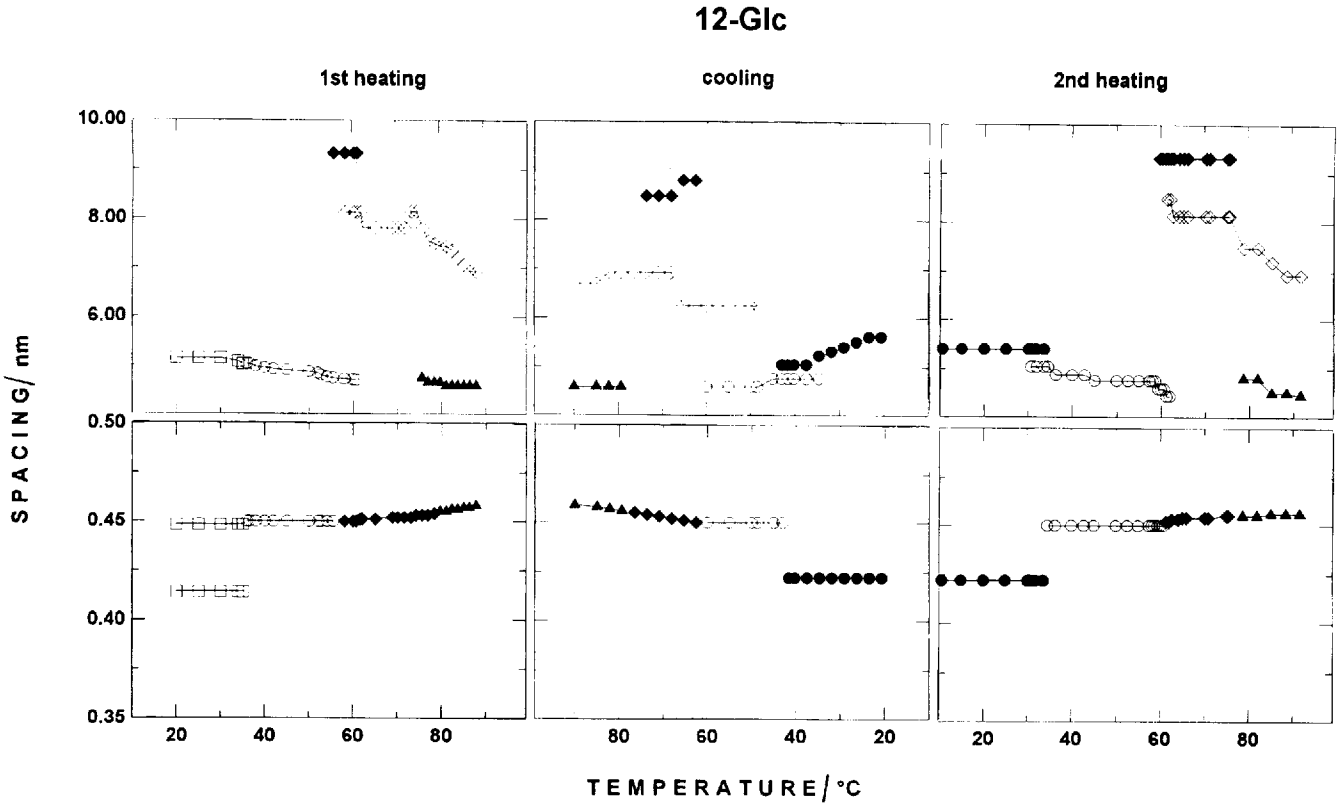

Figure 2. Plots of the low angle (upper row) and wide angle (lower row) X-ray diffraction spacings of 12-Glc during a heating–cooling–heating cycle. The scan rate was 2° min^{-1}. Data acquisition time: 8·5 s/frame. □ lamellar crystalline (L_c) phase; ● lamellar gel (L_β) phase; ○ lamellar liquid crystalline (L_α) phase; ◆, ◇ cubic Q^{229} (*Im*3*m*) and Q^{224} (*Pn*3m) phase, respectively; ▲ hexagonal (H_{II}) phase.

$$\text{2nd heating}\quad \begin{aligned} &\xrightarrow{48^\circ C} L_\alpha \xrightarrow{45^\circ C} L_\alpha + L_\beta \xrightarrow{35^\circ C} L_\beta \\ L_\beta &\xrightarrow{31-34^\circ C} L_\alpha \xrightarrow{60^\circ C} L_\alpha + Q^{229} + Q^{224} \\ &\xrightarrow{62^\circ C} Q^{229} + Q^{224} \xrightarrow{78^\circ C} Q^{224} + H_{II} \end{aligned}$$

According to the diffraction data, after a low-temperature sample preparation the lipid forms a lamellar subgel L_c phase at ambient temperature, with characteristic wide angle reflections at 0·448 nm (major) and 0·414 nm and a lamellar repeat period of 5·15 nm at 20°C (figure 2) [36]. During the initial heating, it melts at about 40°C into a lamellar liquid crystalline L_α phase. In the transition region, the L_c and L_α phases have lamellar repeat periods of 5·03 nm. The transition is identified by the change in the wide angle diffraction pattern to a broad peak at 0·45 nm and also by the precipitous increase of the scattering intensity in the low angle region. Upon further heating, the L_α phase transforms at about 55°C into a non-lamellar phase, with low angle reflections at 6·59, 4·65, 3·82, 3·29, 2·94, 2·69 and 2·48 nm. These reflections appear to index as $1/2^{1/2}:1/4^{1/2}:1/6^{1/2}:1/8^{1/2}:1/10^{1/2}:1/12^{1/2}:1/14^{1/2}$, yielding a lattice basis vector of about 9·32 nm (figure 3). Such a spacing ratio is characteristic of a phase of cubic symmetry, presumably Q^{229} (space group *Im*3*m*) [37]. An alternative identification as space group *Ia*3*d* [26] has also been checked for this pattern. It appears less likely, since the characteristic *Ia*3*d* spacing ratio of $1/6^{1/2}:1/8^{1/2}:1/14^{1/2}:1/16^{1/2}:1/20^{1/2}:1/22^{1/2}$ could hardly be satisfied by the observed reflections. At slightly higher temperature, *c.* 58°C, an additional set of reflections at 5·72, 4·72, 4·10, 3·35, 2·88, 2·70 and 2·57 nm, related in the ratio $1/2^{1/2}:1/3^{1/2}:1/4^{1/2}:1/6^{1/2}:1/8^{1/2}:1/9^{1/2}:1/10^{1/2}$, appear in the low angle diffraction pattern, yielding a lattice basis vector of about 8·12 nm, which could be attributed to another phase of cubic symmetry, possibly Q^{224} (space group *Pn*3*m*) [37] (figure 3). Both sets of non-lamellar reflections coexist in the temperature range 58–61°C, and above 61°C only the *Pn*3*m* cubic phase persists on the low angle diffraction patterns, with a slightly decreased basis vector of 7·81 nm. At about 74°C, an additional three-peak pattern appears with a major peak at 4·75 nm and the other two related to it in the ratio $1:1/3^{1/2}:1/4^{1/2}$, specific for a hexagonal phase. The cubic and hexagonal phases coexist up to the end of the scan at

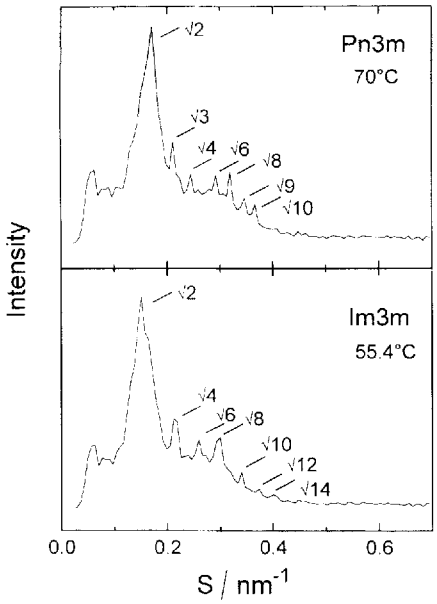

Figure 3. Small angle diffraction patterns of 12-Glc recorded during the 1st heating at 2° min^{-1} in 8·5 s at temperatures 55·4°C and 70·0°C as indicated. According to the reflection spacings ratio, the patterns are assigned to cubic phases, space groups *Im3m* and *Pn3m*, respectively.

90°C, with decreasing low angle spacings upon temperature increase for both of them. The L_α, Q^{229}, Q^{224} and H_{II} phases are detected also in the cooling scan, with the Q^{224} (*Pn3m*) phase coexisting initially with the H_{II} phase, and later on with the Q^{229} and L_α phases. It finally disappears when the first traces of a lamellar gel L_β phase are detected on both low and wide angle diffraction patterns at 45°C. The L_β lamellar repeat spacing is 5·04 nm and gradually increases to 5·61 nm upon temperature decrease to 20°C. According to the low angle diffraction pattern, the L_α and L_β phases coexist in the range 45–35°C. The initial subgel L_c phase is not restored during this cooling protocol, on the timescale of the experiment. The cooling sequence observed is reversible upon subsequent reheating (figure 2, right panels).

3.2. *14-Glc*

1st heating $L_c \xrightarrow{49\text{–}52^\circ C} L_\beta \xrightarrow{54^\circ C} L_\alpha \xrightarrow{56^\circ C} H_{II}$

cooling $H_{II} \xrightarrow{53^\circ C} L_\alpha \xrightarrow{50^\circ C} L_\beta$

2nd heating $L_\beta \xrightarrow{53^\circ C} L_\alpha \xrightarrow{55^\circ C} H_{II}$

At low temperatures, at the beginning of the 1st heating run, the lipid is in the lamellar crystalline L_c phase characterized by a lamellar repeat period of 5·50 nm and wide angle diffraction bands at 0·442 nm (major) and 0·381 nm (figure 4). Upon heating, it converts into the lamellar gel L_β phase with hexagonally arranged hydrocarbon chains (wide angle reflection at 0·419 nm) and lamellar repeat period of 5·65 nm. The two phases coexist between about 49°C and 52·5°C, as manifested by the wide angle pattern. The L_β phase is a narrow range intermediate which rapidly transforms into a lamellar liquid crystalline phase upon further heating, at about 54°C. This transformation is accompanied by a decrease in the lamellar period to 5·55 nm and a change in the wide angle pattern to a broad reflection centred at 0·442 nm. At 56°C, the L_α phase converts to a hexagonal phase, with the characteristic low angle spacings ratio of $1:1/3^{1/2}:1/4^{1/2}$, with the first order reflection at 6·20 nm. The lamellar and the hexagonal phases are seen to coexist in the low angle patterns of several sequential frames. Upon further heating, the spacing of the hexagonal phase decreases and at 80°C the 1st order reflection is at 5·50 nm. This thermal change is reversible upon cooling—the H_{II} phase spacing is 6·08 nm just before its conversion back into the L_α phase at 53°C. The $L_\alpha \rightarrow L_\beta$ conversion takes place at about 50°C. No more phase changes occur in this lipid upon further cooling to 25°C. No restoration of the initial L_c phase takes place for several hours. The cooling phase sequence is reversible upon immediate reheating with a temperature hysteresis of about 3°C for the $L_\beta \rightarrow L_\alpha$ transition and about 2°C for the $L_\alpha \rightarrow H_{II}$ transition.

3.3. *16-Glc*

1st heating $L_c \xrightarrow{50^\circ C} L_\beta \xrightarrow{63^\circ C} H_{II}$

cooling $H_{II} \xrightarrow{62^\circ C} L_\beta$

2nd heating $L_\beta \xrightarrow{63^\circ C} H_{II}$

This lipid has not been previously studied by X-ray diffraction. After low-temperature sample preparation, at 20°C this lipid is also in the lamellar crystalline state with lamellar period of 5·60 nm and wide angle reflections at 0·435 and 0·392 nm (figure 5), similar to those of 14-Glc. The structural characteristics of this phase do not change upon heating to 50°C. At 50–51°C, the wide angle pattern changes to a single reflection at 0·418 nm. An increase in the lamellar period to 6·15 nm accompanies the change in the wide angle picture and at 52°C the diffraction pattern is typical for a lamellar gel L_β phase. It undergoes a direct conversion into a hexagonal phase between 61·5° and 63·5°C, via a two-state process, with a phase coexistence range of about 2°C. The hexagonal phase *d*-spacing is 5·52 nm and it slightly decreases upon heating to 70°C. Upon cooling and immediate reheating, in the temperature range 30–70°C, a reversible interconversion between the L_β and the H_{II} phases takes place at 61·5°C on cooling and at 63°C on reheating. The initial lamellar crystalline phase is not restored on the timescale of the experiment.

3.4. *18-Glc*

1st heating $L_c \xrightarrow{59°C} L_\beta \xrightarrow{70°C} H_{II}$

cooling $H_{II} \xrightarrow{70°C} L_\beta$

2nd heating $L_\beta \xrightarrow{70°C} H_{II}$

The phase sequences in this lipid coincide with those of 16-Glc, with differences in the transition termperatures. At low temperature, this lipid is also in the lamellar crystalline phase with lamellar period of 6·08 nm and wide angle reflections at 0·442 and 0·382 nm at 20°C (figure 6). The structural characteristics of this phase do not change upon heating. At 58°C a new wide angle band appears at 0·418 nm and increases in intensity upon heating, while the initial two bands decrease. An increase in the lamellar period to 6·68 nm accompanies these changes in the wide angle pattern and at 60°C the diffraction pattern is typical of a lamellar gel L_β phase. It undergoes a conversion into a hexagonal phase between 69° and 70°C with a phase coexistence range of about 1°C. The *d*-spacing of the hexagonal phase is 5·85 nm and it decreases progressively upon heating to 80°C. Upon cooling and reheating, a single phase transition takes place in the temperature range 20–80°C. This is a reversible interconversion between the L_β and the H_{II} phases at 70°C on cooling and at 70·5°C on reheating. The initial lamellar crystalline phase is not restored on the timescale of the experiment.

3.5. *14-Gal*

1st heating $L_{c1} \xrightarrow{55–60°C} L_{c2} \xrightarrow{64–72°C} H_{II}$

cooling $H_{II} \xrightarrow{62–57°C} L_\alpha \xrightarrow{47°C} L_\beta \xrightarrow{37°C} L_{c2}$

2nd heating $L_{c2} \xrightarrow{70°C} H_{II}$

At the beginning of the 1st heating, at 40°C, 14-Gal is in lamellar crystalline phase, L_{c1}, with repeat spacing of 5·48 nm and wide angle reflections at 0·348, 0·392 and 0·448 nm (figure 7). Upon heating, this phase converts into another crystalline modification, L_{c2}, with the same lamellar period and a different set of wide angle reflections at 0·392, 0·378, 0·435 and 0·448 nm. The transformation takes place between 55 and 60°C, with the two modifications coexisting in this range. No anomalies in the heat capacity were found to be associated with this conversion [13]. At about 70°C, a major restructuring of the lipid bilayers takes place and a hexagonal liquid crystalline phase forms directly from the lamellar crystalline phase. The L_c and H_{II} phases coexist in a relatively

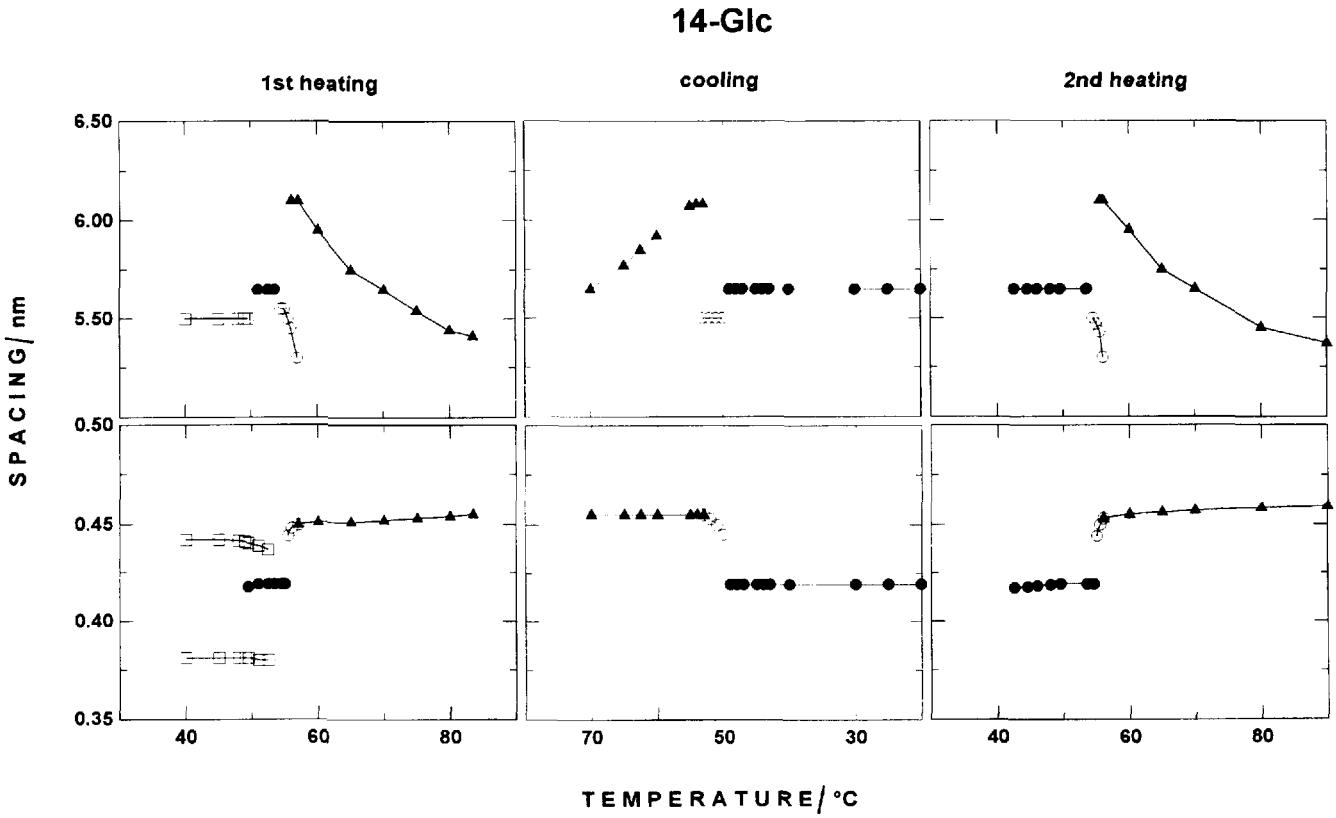

Figure 4. Plots of the low angle (upper row) and wide angle (lower row) X-ray diffraction spacings of 14-Glc collected during a heating-cooling-heating cycle. The scan rate was 5° min^{-1}. Data acquisition time: 2 s/frame. Symbols as in figure 2.

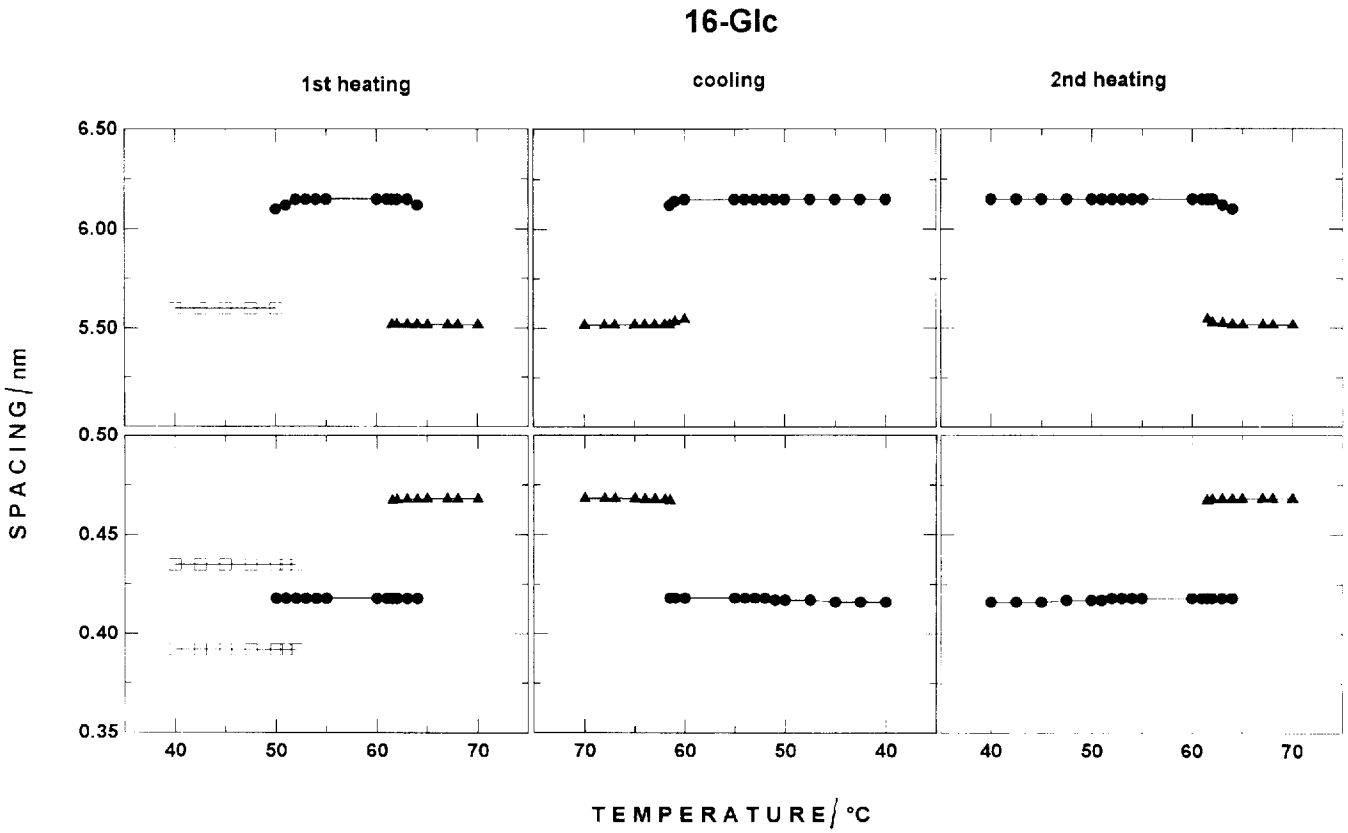

Figure 5. Plots of the low angle (upper row) and wide angle (lower row) X-ray diffraction spacings of 16-Glc collected during a heating–cooling heating cycle at 2° min^{-1} scan rate. Data acquisition time 3 s/frame. Symbols as in figure 2.

broad temperature range from 64 to 72°C. In this range, the low angle spacing of the H_{II} phase coincides with the lamellar repeat period of the L_c phase — 5·48 nm — and slightly decreases upon further heating. The direct $L_c \rightarrow H_{II}$ transition on heating is replaced by a complicated pathway upon the subsequent cooling, which includes L_α and L_β intermediates. The low angle spacing of the H_{II} phase sharply increases to more than 6 nm during the $H_{II} \rightarrow L_\alpha$ transformation, which takes place in the temperature range 62–57°C. The lamellar period of the L_α phase also increases in the transition region from 4·87 up to 5·07 nm. Upon cooling to lower temperatures, at about 47°C the L_α phase converts to L_β with a lamellar period of 5·52 nm. The wide angle diffraction spacings of both L_α and L_β phases are seen to decrease upon cooling, with slopes of about 10^{-3} nm $°C^{-1}$ for the L_α phase and $6 \cdot 10^{-4}$ nm $°C^{-1}$ for the L_β phase, respectively. At 37°C, the subgel phase L_{c2} starts to recover, as seen from the wide angle diffraction pattern (figure 8). Subsequent reheating displays a direct $L_{c2} \rightarrow H_{II}$ transition.

3.6. *14-2,3-Gal*

1st heating $L_c \xrightarrow{58°C} L_\alpha \xrightarrow{63°C} H_{II}$

cooling $H_{II} \xrightarrow{62°C} L_\alpha \xrightarrow{51°C} L_\beta$

2nd heating $L_\beta \xrightarrow{53°C} L_\alpha \xrightarrow{64°C} H_{II}$

The lipid initially forms a lamellar subgel L_c phase, characterized by two wide angle reflections at 0·442, 0·392 nm and a 5·6 nm lamellar repeat period (figure 9). This phase melts at about 58°C into a lamellar liquid crystalline L_α phase, with a repeat distance of 5·25 nm. Upon further heating, it transforms at about 63°C into a hexagonal phase, with a 1st order low angle spacing of 5·84 nm at 64°C. The $L_\alpha \rightarrow H_{II}$ transition is reversible on cooling with a hysteresis of about 1°C, but the initial subgel phase does not restore upon further cooling. A gel L_β phase with a single wide angle band at 0·418 nm and lamellar period of 5·8 nm is formed instead at 51°C. The cooling phase sequence is reversible on heating, with no restoration of the initial lamellar subgel phase observed during the duration of the experiments (several hours).

3.7. *18-Gal*

1st heating $L_{c1} \xrightarrow{57–72°C} L_{c2} \xrightarrow{71–84°C} H_{II}$

cooling $H_{II} \xrightarrow{67°C} L_\beta$

2nd heating $L_\beta \xrightarrow{60–72°C(exo)} L_c \xrightarrow{72–85°C} H_{II}$

The phase sequence during the first heating of this lipid is similar to that of 14-Gal interconversion between

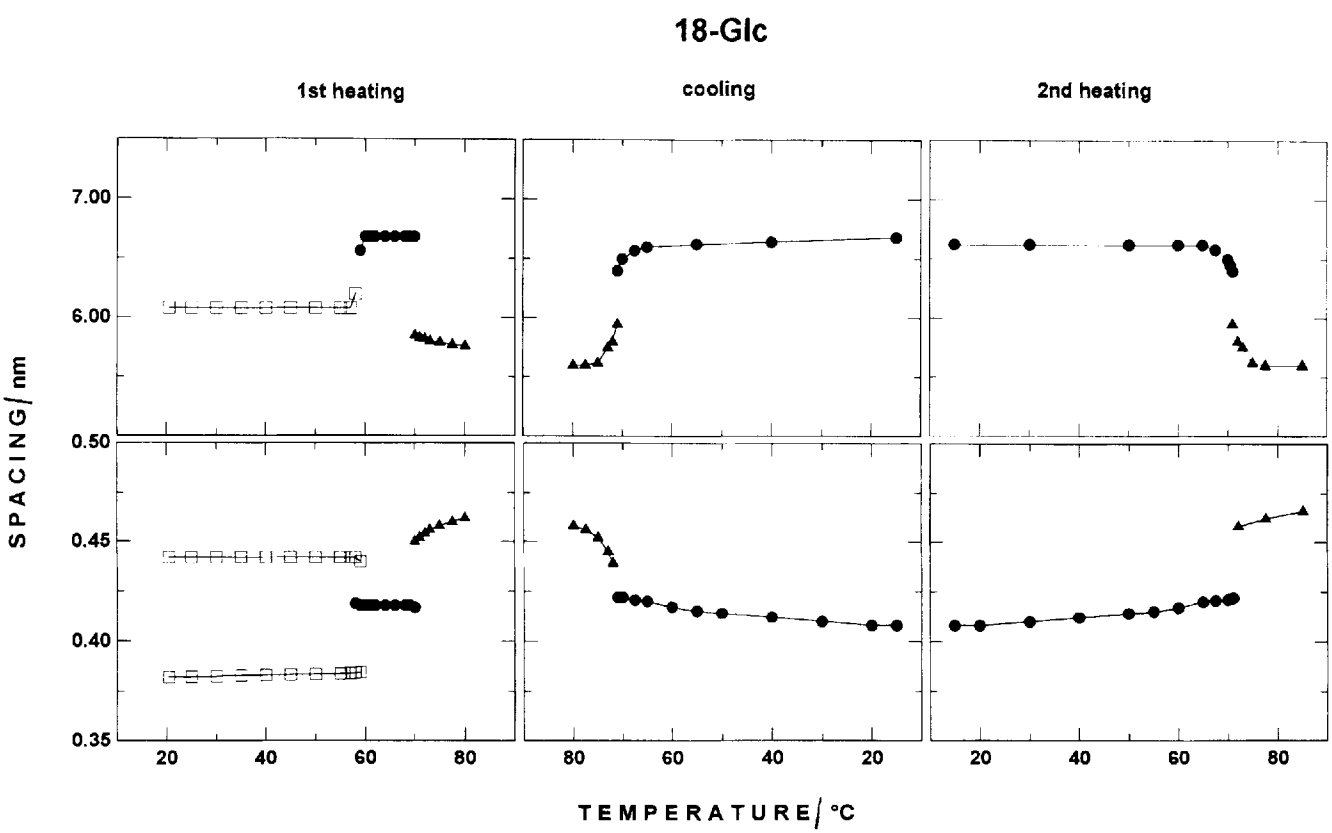

Figure 6. Plots of the low angle (upper row) and wide angle (lower row) X-ray diffraction spacings of 18-Glc collected during a heating-cooling-heating cycle at 5° min^{-1} scan rate. Data acquisition time 2 s/frame. Symbols as in figure 2.

two lamellar crystalline modifications taking place in a wide temperature range (57–72°C), followed by a direct subgel→H_{II} transition (figure 10). The latter transition also proceeds via phase coexistence in a broad temperature range (71–84°C). In this range the low angle spacing of the H_{II} phase (5·90 nm) does not change, but after the final disappearance of the subgel phase it decreases upon further heating and is 5·50 nm at 90°C. However, the cooling phase sequence is different from that of 14-Gal; the L_α phase is missing and a direct, H_{II}→L_β transition takes place at about 67°C. The lamellar period of the L_β phase of 6·55 nm does not change upon cooling to 30°C. The spacing of its wide angle diffraction peak decreases from 0·419 nm at 65°C to 0·408 nm at 30°C. Upon immediate reheating, the L_β phase persists up to 60°C. Above this temperature, a spontaneous crystallization into a highly ordered subgel phase is initiated, and at 72°C the lipid is fully converted into a subgel state with major wide angle reflections coinciding with those of the L_{c2} phase (figure 11). According to the low angle diffraction pattern, it starts immediately to convert into the H_{II} phase. This conversion also proceeds within an extended phase coexistence region (72–85°C).

3.8. *16-Man*

1st heating $L_\beta \xrightarrow{61°C} H_{II}$

cooling $H_{II} \xrightarrow{61°C} L_\beta$

2nd heating $L_\beta \xrightarrow{61°C} H_{II}$

The phase behaviour of this lipid during heating-cooling cycles is very simple; a reversible direct L_β→H_{II} transition takes place at 61°C, practically without temperature hysteresis. The two phases coexist in a temperature interval of about 1°C (figure 12). The low angle spacing of the H_{II} phase decreases from 5·65 nm at 62°C to 5·00 nm at about 80°C.

4. Discussion

4.1. *Conversions between lamellar solid phases of glycoglycerolipids*

The dialkylglycoglycerolipids examined here have been studied previously by differential scanning calorimetry, scanning densitometry and, except for 16-Glc, by static X-ray diffraction [7–9, 12, 13, 23, 24, 26, 28]. The structural characterization provided here for 16-Glc (figure 5 and table) shows identical phase sequences in this lipid and 18-Glc, involving an irreversible subgel-gel

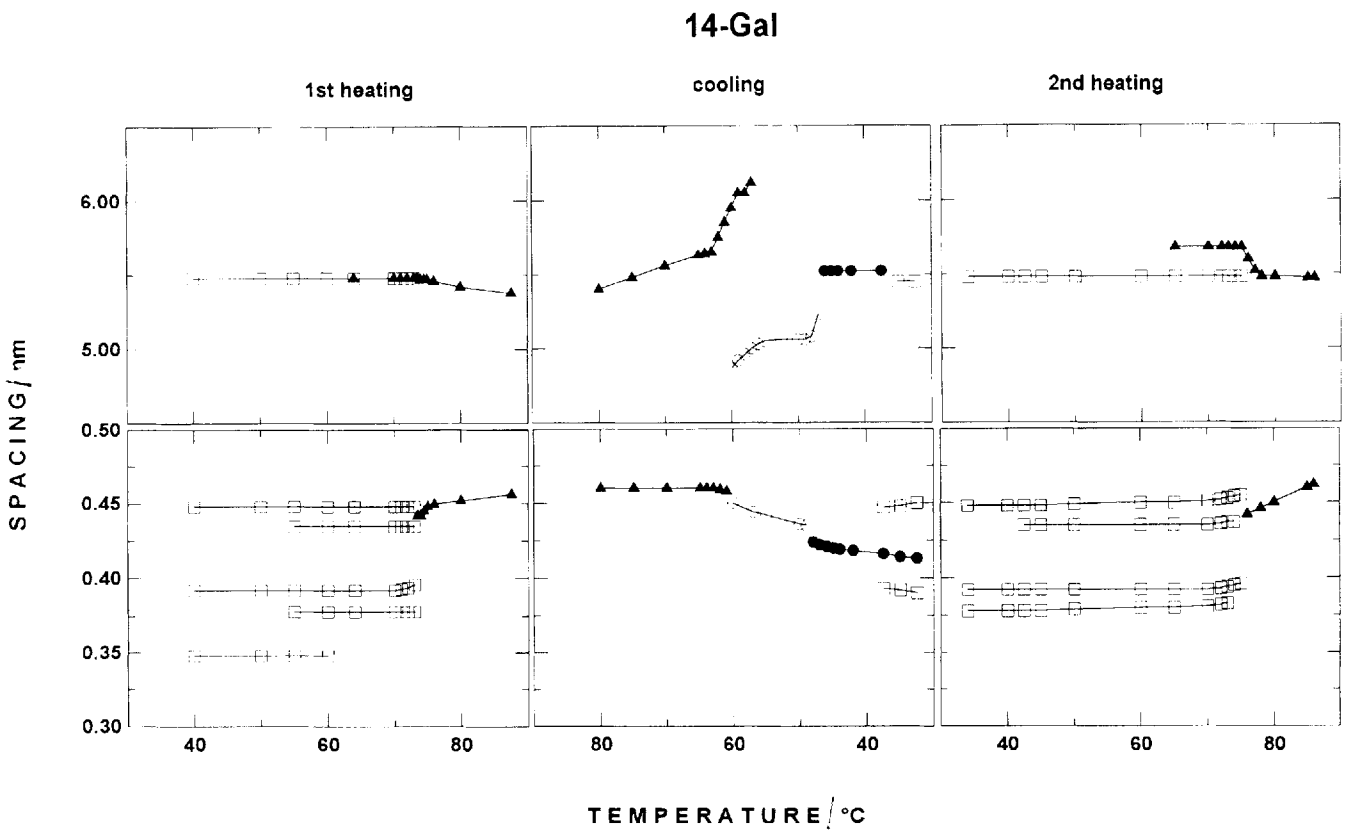

Figure 7. Plots of the low angle (upper row) and wide angle (lower row) X-ray diffraction spacings of 14-Gal during a heating–cooling–heating cycle at 5° min^{-1} scan rate. Data acquisition time 2 s/frame. Symbols as in figure 2.

transition and direct, fully reversible lamellar gel-inverted hexagonal phase transformation.

The present study provides new information concerning detailed transition pathways and reversibility in short chain glycoglycerolipids. Their phase sequences represent collections of nearly all phases found in double chain lipids, e.g. 12-Glc (figure 2); 14-Glc (figure 4); 14-Gal, cooling (figure 7, middle panels). Intermediate lamellar gel phases in 14-Glc and 14-Gal, not detected earlier, have been observed in the present study. In 14-Glc, a lamellar gel intermediate has been detected in a temperature range of about 2°C between the lamellar subgel and lamellar liquid crystalline phases during the first heating (figure 4). Also, the cooling sequence of 14-Gal includes two metastable structures absent in heating scans; the transformation from the hexagonal liquid crystalline into the lamellar subgel phase proceeds via lamellar liquid crystalline and lamellar gel intermediates in this lipid (figure 7, middle panels).

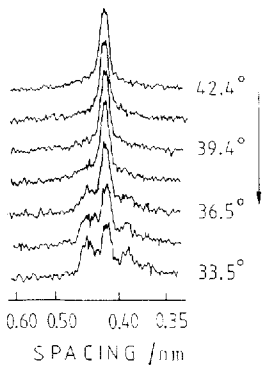

Figure 8. Wide angle diffraction patterns of 14-Gal recorded during cooling at a 5° min^{-1} scan rate. Scattering intensities recorded in 2 s are shown at the temperatures as indicated.

The structural background of the exotherm present in second and subsequent heating thermograms of 18-Gal [13, 23] is identified in the present study as spontaneous crystallization of the metastable lamellar gel phase (figures 10, 11). Fast spontaneous exothermic conversion between metastable and stable phases upon heating, although infrequent in lipids, has been observed to take place also in another class of long chain galactolipids-*N*-galactosylsphingosines (cerebrosides) with 16 and 24 carbon atoms in the fatty acid chain [40, 41]. This obviously indicates a strongly decreased life-time of the L_β phase of

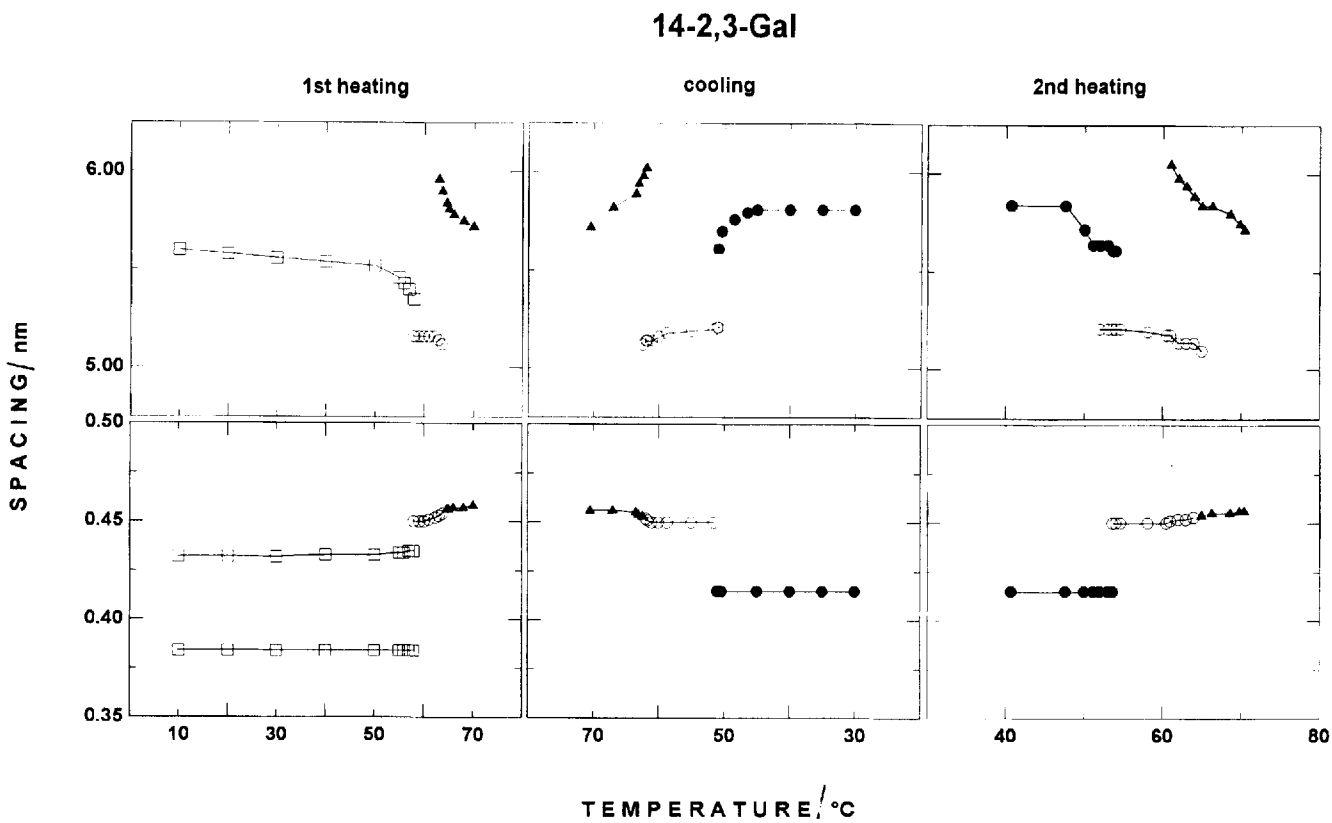

Figure 9. Plots of the low angle (upper row) and wide angle (lower row) X-ray diffraction spacings of 14-2,3-Gal during a heating-cooling-heating cycle at 5° min^{-1} scan rate. Data acquisition time 2 s/frame. Symbols as in figure 2.

18-Gal at temperatures immediately below the melting $L_c \rightarrow H_{II}$ transition. An exothermic transition has been recorded by calorimetry also in 16-Gal, but not in 14-Gal [13, 23]. This is consistent with the X-ray data in figure 7, which show that the $L_\beta \rightarrow L_c$ conversion takes place in 14-Gal during the cooling scan. Conversions between the subgel modifications of 14-Gal and 18-Gal species proceed in broad temperature ranges (figures 7, 10). Although easily discernible from the wide angle diffraction patterns, they are not accompanied by detectable anomalies in the heat capacity [13, 23].

4.2. *Properties of the lamellar–inverted hexagonal phase transitions in glycoglycerolipids*

All the glycoglycerolipids examined here form the inverted hexagonal phase at high temperatures. In five of them (16-Glc, 18-Glc, 14-Gal, 18-Gal, 16-Man) the hexagonal phase appears through a direct transformation from a lamellar gel or subgel phase. In all cases, the lamellar→hexagonal phase transitions proceed as two-state processes, with clearly distinguished phase coexistence and absence of detectable intermediate structures.

A remarkable property of the 1,2-dialkylmonogalactosides is their ability to undergo direct subgel–inverted hexagonal phase transitions (figures 7, 10). Conversions of this type have not been detected in other lipid/water systems. The properties of the $L_c \rightarrow H_{II}$ transitions significantly differ from those of the $L_\beta \rightarrow H_{II}$ and $L_\alpha \rightarrow H_{II}$ transitions in the following respects. They are characterized by extended coexistence regions, a likely result of slow transition kinetics, and by constant lattice parameters not only of the L_c, but also of the H_{II} phase thoughout the transition region. Immediately above the coexistence region, the H_{II} lattice rapidly shrinks to a smaller value (figures 7, 10). After that, the spacing continues to decrease slowly, according to its temperature compressibility. Another noteworthy distinction is that, according to the present data, a transformation from a highly ordered subgel phase directly into a hexagonal liquid crystalline phase is possible in the heating direction only. Significant differences in the transition pathways for these glycolipids have been distinguished in the cooling direction. The lamellar L_β and L_α phases omitted in the heating phase sequence, may appear in cooling scans. In the case of 14-Gal, the direct $L_c \rightarrow H_{II}$ transition on heating is replaced by an $H_{II} \rightarrow L_\alpha \rightarrow L_\beta \rightarrow L_c$

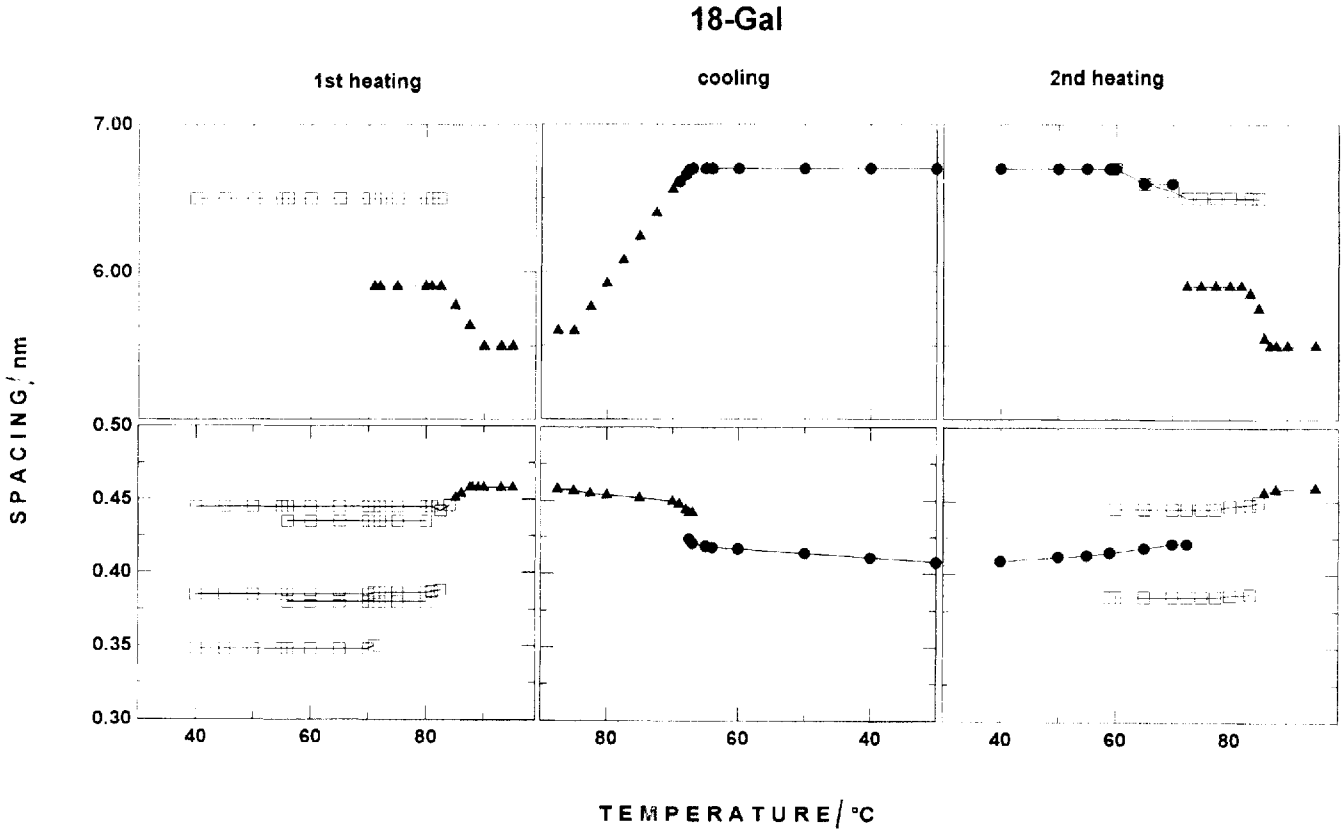

Figure 10. Plots of the low angle (upper row) and wide angle (lower row) X-ray diffraction spacing of 18-Gal during a heating-cooling-heating cycle at 5° min^{-1} scan rate. Data acquisition time 2 s/frame. Symbols as in figure 2.

sequence on cooling (figure 7). With 18-Gal, the $L_c \rightarrow H_{II}$ transition on heating is replaced by a $H_{II} \rightarrow L_\beta$ transition on cooling, with the L_β phase as a long lived metastable intermediate which becomes unstable and spontaneously converts into L_c in a temperature range immediately below the $L_c \rightarrow H_{II}$ transition (figure 10).

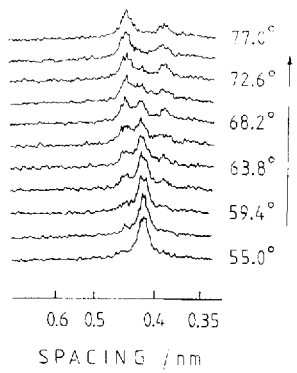

Figure 11. Wide angle diffraction patterns of 18-Gal recorded during the 2nd heating at 5° min^{-1}. Scattering intensities recorded in 2 s are shown at the temperatures indicated.

By contrast with the $L_c \rightarrow H_{II}$ transitions, the direct gel-hexagonal phase transitions recorded in 16-Glc, 18-Glc and 16-Man, are fully reversible, with very small or absent temperature hysteresis (figures 5, 6, 12). The $L_\beta \leftrightarrow H_{II}$ transitions in 18-Glc (figure 6) and 16-Man (figure 12) proceed at the same temperature in either direction, practically without temperature hysteresis, even at a relatively high scan rate of 5°C min^{-1}. In 16-Glc, the $L_\beta \leftrightarrow H_{II}$ transition proceeds with a hysteresis of about 1°C at a scan rate of 2°C min^{-1} (figure 5). For comparison, the temperature hysteresis in $L_\alpha \leftrightarrow H_{II}$ transitions is typically in the range 2–3°C. For the direct $L_\beta \leftrightarrow H_{II}$ transitions in 16-Glc, 18-Glc, and 16-Man, the lamellar repeat period of the L_β phase exceeds within less than 3–4% the lattice parameter $a = 2d/3^{1/2}$ of the H_{II} phase at the transition temperature (see the table). The close coincidence of the structural parameters may mean that no large spatial rearrangement of lipid and water takes place in this transition and thus might be the origin of the precise reversibility of the $L_\beta \leftrightarrow H_{II}$ transition. Similar minor temperature hysteresis and coinciding structural parameters at the transition temperature also characterize the direct $L_\beta \leftrightarrow H_{II}$ transition in the mixture

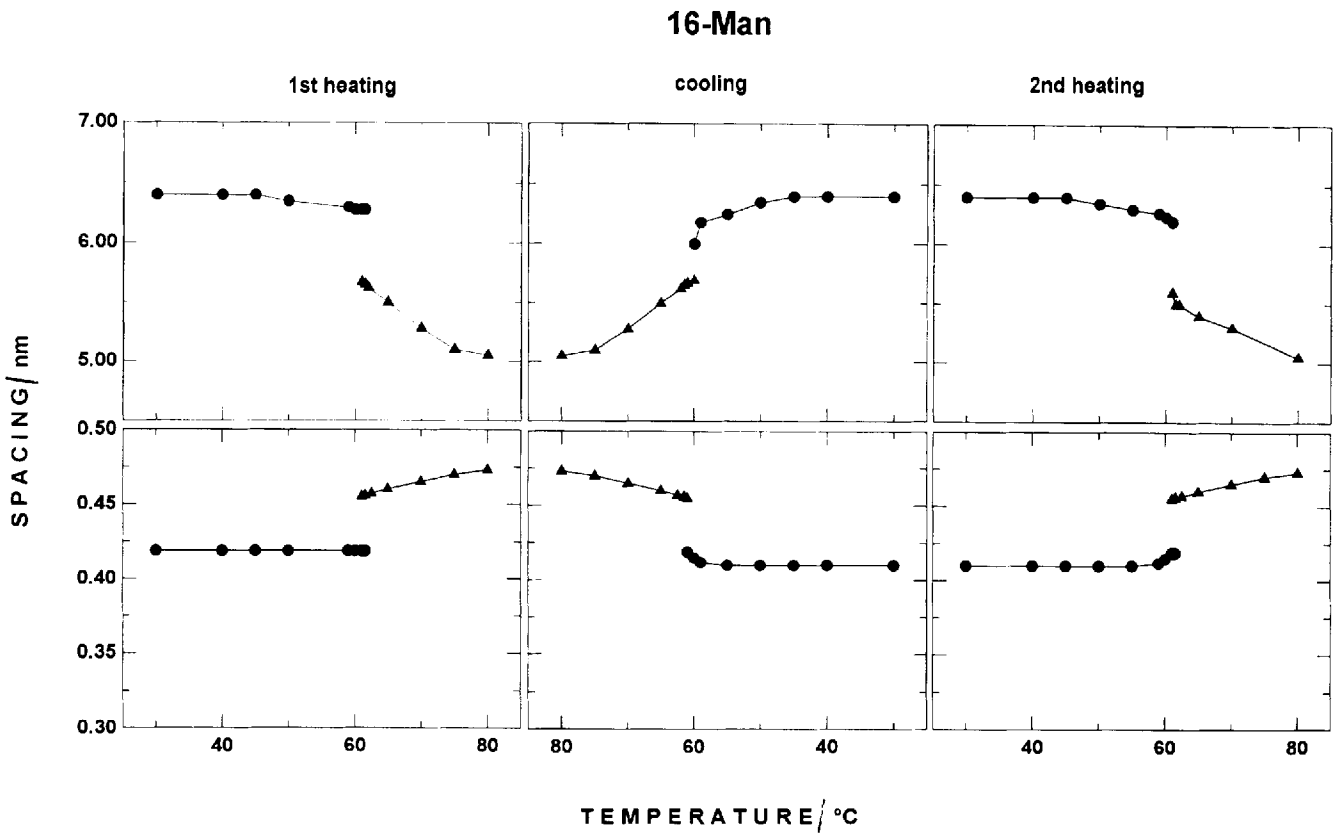

Figure 12. Plots of the low angle (upper row) and wide angle (lower row) X-ray diffraction spacings of 16-Man during a heating-cooling-heating cycle at 5° min^{-1} scan rate. Data acquisition time 2 s/frame. Symbols as in figure 2.

dipalmitoylphosphatidylcholine/palmitic acid (1:2, mol/mol) [42, 43].

In $L_\alpha \rightarrow H_{II}$ transitions, a considerable decrease of the low angle *d*-spacing for both L_α and H_{II} phases is observed in the temperature range of their coexistence, e.g. 14-Glc (figure 4), 14-Gal cooling (figure 7, middle panels), 14-2,3-Gal (figure 9). A smaller decrease of the *d*-spacings is present also in the $L_\beta \rightarrow H_{II}$ transitions of 16-Glc (figure 5), 18-Glc (figure 6) and 16-Man (figure 12).

4.3. *Phase transformations including cubic phases*

In 12-Glc, the phase sequence includes two distinct cubic phases between the L_α and H_{II} phases. Our present data are consistent with a tentative assignment of these phases as belonging to space groups *Im3m* and *Pn3m*. This assignment needs, however, further verification. It is noteworthy that these two cubic phases appear in the same sequence upon heating of aqueous dispersions of another glycerolipid, didodecylphosphatidylethanolamine, with identical alkyl chain length and glycerol backbone [38, 39]. A comparison of the phase transition temperatures of 12-Glc and didodecylphosphatidylethanolamine shows that replacement of the monoglucoside head group with a phosphorylethanolamine moiety does not alter significantly the temperature of the melting $L_c \rightarrow L_\alpha$ transition, but results in a substantial increase of the temperature of the $L_\alpha \rightarrow Q_{II}$ transition by more than 35°C. Cubic phases of space groups *Im3m* and *Pn3m* have also been found to coexist in aqueous dispersions of dioleoylphosphatidylethanolamine after intensive temperature cycling [51]. Upon heating, the *Im3m* phase disappears at about 45°C, while *Pn3m* is stable up to about 75°C. Prolonged equilibrium of *N*-methylated dioleoylphosphatidylethanolamine at a temperature just below the $L_\alpha \rightarrow H_{II}$ transition also results in formation of coexisting *Im3m* and *Pn3m* phases [45]. The *Im3m* and *Pn3m* phases seem to be the phases of cubic symmetry which have been up to now usually observed to form in fully hydrated two chain lipids. At low water contents, two chain lipids typically form cubic phases of the space group *Ia3d* (see, e.g. [46]).

The *Pn3m* phase strongly undercools, practically until the conversion to the lamellar gel phase (figure 2). The ability of the cubic phases to undercool, once accessed, is well known from previous studies and, supposedly, originates from slow water release taking place during the cubic→lamellar transformation [45–47].

Table. Low angle spacings d (nm) of the glycolipid phases at the indicated temperatures, and also at their appearance (superscript i) and disappearance (superscript f) upon heating; the lattice parameter, $a = 2d/3^{1/2}$ of the inverted hexagonal (H_{II}) phase is shown in brackets.

Phase	12-Glc	14-Glc	16-Glc	18-Glc	14-Gal	14-2,3-Gal	18-Gla	16-Man
L_c (35–40°C)	5·03	5·50	5·60	6·08	5·48	5·54	6·50	•[a]
L_c^f	5·03	5·50	5·60	6·20	5·48	5·35	6·50	•
L_α^i	5·40	5·65	6·10	6·56	5·52[b]	5·84	6·70	6·40
L_β (35–40°C)	5·40	5·65	6·15	6·62	5·52	5·84	6·70	6·40
L_β^f	5·40	5·65	6·12	6·68	5·52[b]	5·61	6·60	6·28
L_α^i	5·03	5·55	•	•	5·23[b]	5·16	•	•
L_α (~55°C)	4·76	5·40	•	•	5·05	5·16	•	•
L_α^f	4·70	5·30	•	•	4·87[b]	5·12	•	•
Q^{229} (60°C)	9·32	•	•	•	•	•	•	•
Q^{224i}	8·12	•	•	•	•	•	•	•
Q^{224} (70°C)	7·81	•	•	•	•	•	•	•
Q^{224} (90°C)	6·93	•	•	•	•	•	•	•
H_{II}^i	4·75	6·20	5·52	5·85	5·48	5·96	5·90	5·67
	(5·48)	(7·16)	(6·37)	(6·75)	(6·33)	(6·88)	(6·81)	(6·55)
H_{II} (70–75°C)	4·75	5·65	5·52	5·79	5·47	5·72	5·90	5·10
	(5·48)	(6·52)	(6·37)	(6·69)	(6·32)	(6·60)	(6·81)	(5·89)
H_{II} (100°C)[c]	4·63	5·30	5·51	5·75				
	(5·48)	(6·52)	(6·37)	(6·69)				

[a] phases absent in these lipids marked •
[b] lamellar repeat periods taken from the cooling sequence
[c] values of d determined by extrapolation to 100°C

4.4. *Effect of temperature and chain length on the lattice parameters of the inverted hexagonal phase*

The thermal shrinking of the H_{II} lattice outside the transition region is expressed in a lattice spacing decrease by $\sim -0{\cdot}01$ to $-0{\cdot}03$ nm °C^{-1}. A decrease of similar magnitude of the H_{II} lattice spacing ($\sim -0{\cdot}02$ nm °C^{-1}) has been observed in aqueous dispersions of phosphatidylethanolamines [34, 35, 44]. It has been shown to result from progressively smaller water core radii as the temperature is increased [34]. The *Pn3m* cubic phase formed in 12-Glc exhibits even stronger thermal shrinking of $\sim -0{\cdot}04$ to $-0{\cdot}05$ nm °C^{-1} (figure 2).

In order to demonstrate the effect of chain length, the low angle X-ray spacings of the different phases are plotted in figure 13 as a function of chain length for the series of 1,2-dialkylmonoglucosides with 12, 14, 16, and 18 carbon atoms in the alkyl chains. For the L_c and L_β phases this dependence is close to linear, with increments per CH_2 group of 0·162 nm for the L_c phase, and 0·208 nm for the L_β phase. For the H_{II} phase, however, the dependence of the lattice parameter on the chain length strongly deviates from linearity and has a maximum at a chain length of 14 carbon atoms. This maximum coincides with a dramatic change in the phase behaviour at this chain length: (i) no cubic phases form in 14-Glc; (ii) an L_β phase intervenes during heating at this chain length and the L_α phase disappears upon chain elongation above 14 carbon atoms. The anomalously high spacing of the hexagonal phase in 14-Glc thus appears to be connected with the substantially bigger lattice parameters of the cubic phases in 12-Glc (dashed lines in figure 13). The chain elongation from 12 to 14 carbon atoms results in inability of 14-Glc to form cubic phases, at least under experimental protocols of a few heating and cooling scans. The H_{II} phase in 14-Glc retains, however, a high lattice parameter characteristic of the cubic phases. This expanded phase gradually relaxes to a 'normal' hexagonal phase upon further heating. Correspondingly, the maximum in the H_{II} phase lattice parameter at 14 carbon atoms is best expressed at temperatures immediately after H_{II} formation and almost disappears upon extrapolation to 100°C (figure 13 and table).

As mentioned above, a noteworthy analogy exists between the behaviour of the alkyl chain monoglucosides studied here, and alkyl chain phosphatidylethanolamines. Similarly to the monoglucosides, chain elongation from 12 to 14 carbon atoms results in inability of these phosphatidylethanolamines to form cubic phases [52]. In addition, the dependence of the lattice par-

ameters of their L_c, L_β and L_α phases on the chain length is also linear, while for the H_{II} phase it deviates from linearity [44].

The relatively big lattice parameter of the H_{II} phase immediately above the $L_\alpha \rightarrow H_{II}$ transition in 14-Glc indicates a weaker propensity of this lipid to assume non-bilayer configurations [45]. According to the notion of intrinsic curvature of the lipid bilayers [48], this can be classified as an example of intermediate curvature between curvatures characterizing the H_{II} phases in 16- and 18-Glc and curvatures of lipids which do not form non-bilayer phases. Lipids of such intermediate intrinsic curvature are known to exhibit slow and complicated non-equilibrium phase behaviour [49, 50]. It is thus conceivable that specific temperature treatment of 14-Glc, such as temperature cycling or long incubation at temperatures near the $L_\alpha \rightarrow H_{II}$ transition, may result in formation of cubic intermediates between the L_α and H_{II} phases. Our preliminary calorimetric data provide support for this assumption.

Financial support from the Bulgarian Academy and the Bulgarian National Science Foundation, grant K-407/1994, (R.T. and B.T.), Deutsche Forschungsgemeinschaft, and the Royal Society are gratefully acknowledged. The authors are indebted to Dr Helmut Kuttenreich for the glycolipid synthesis. Assistance of Wim Bras of the Daresbury Laboratory was provided for dynamic X-ray diffraction measurements.

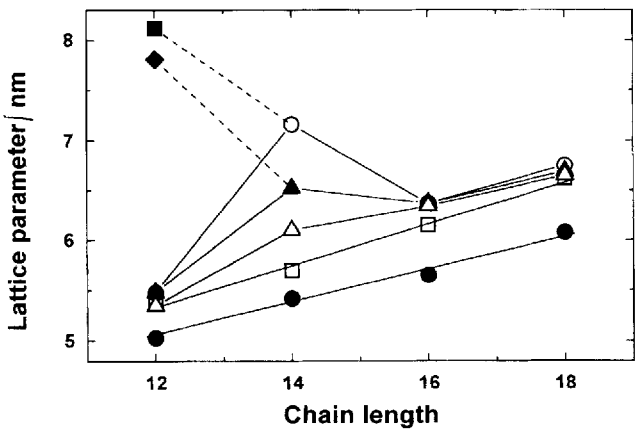

Figure 13. Dependence of the lattice parameters on the chain length for the series of 1,2-dialkylglucosides; ● lamellar crystalline (L_c) phase repeat period at 35–40°C; □ lamellar gel (L_β) phase repeat period at 35–40°C; ○ hexagonal (H_{II}) phase lattice parameter $a = 2d/3^{1/2}$ at the temperature of its appearance upon heating; ▲ hexagonal (H_{II}) phase lattice parameter at 75–80°C; △ hexagonal (H_{II}) phase lattice parameter as extrapolated to 100°C; ◆ cubic (Q^{224}) phase lattice parameter (low angle 1st order spacing) at 70°C; ■ cubic (Q^{224}) phase lattice parameter (low angle 1st order spacing) at the temperature of its appearance upon heating.

References

[1] Quin, P. J., and Williams, W. P., 1978, *Prog. Biophys. Mol. Biol.*, **34,** 109.
[2] Ishizuka, I., and Yamakawa, T., 1985, *Glycolipids (New Comprehensive Biochemistry)*, edited by H. Wiegandt, Vol. 10 (New York: Elsevier Acad. Press), p. 101.
[3] Koynova, R., and Caffrey, M., 1994, *Chem. Phys. Lipids*, **69,** 181.
[4] Endo, T., Inoue, K., and Nojima, S., 1982, *J. Biochem. (Tokyo)*, **92,** 953.
[5] Six, L., Ruess, K., and Lieflander, M., 1983, *Tetrahedron Lett.*, **24,** 1229.
[6] Jarrell, H. C., Jovall, P. E., Giziewicz, J. B., Turner, L. A., and Smith, I. C. P., 1987, *Biochemistry*, **26,** 1805.
[7] Hinz, H.-J., Six, L., Ruess, K., and Lieflander, M., 1985, *Biochemistry*, **24,** 806.
[8] Kuttenreich, H., 1992, PhD thesis, University of Regensburg.
[9] Blocher, D., Six, L., Gutermann, R., Henkel, B., and Ring, K., 1985, *Biochim. Biophys. Acta*, **818,** 313.
[10] Carrier, D., Giziewicz, J., Moir, D., Smith, I., and Jarrell, H. C., 1989, *Biochim. Biophys. Acta*, **983,** 100.
[11] Jarrell, H. C., Wand, A., Giziewicz, J. B., and Smith, I. C. P., 1987, *Biochim. Biophys. Acta*, **897,** 69.
[12] Koynova, R., Kuttenreich, H., Tenchov, B., and Hinz, H.-J., 1988, *Biochemistry*, **27,** 4612.
[13] Kuttenreich, H., Hinz, H.-J., Inczedy-Marcsek, M., Koynova, R., Tenchov, B., and Laggner, P., 1988, *Chem. Phys. Lipids*, **47,** 245.
[14] Mannock, D. A., Lewis, R. N. A. H., Sen, A., and McElhaney, R. N., 1988, *Biochemistry*, **27,** 6852.
[15] Renou, J.-P., Giziewicz, J., Smith, I., and Jarrell, H., 1989, *Biochemistry*, **28,** 1804.
[16] Mannock, D. A., Lewis, R. N. A. H., and McElhaney, R. N., 1990, *Chem. Phys. Lipids*, **55,** 309.
[17] Asgharian, B., Cadenhead, D. A., Mannock, D. A., Lewis, R. N. A. H., and McElhaney, R. N., 1989, *Biochemistry*, **28,** 7102.
[18] Auger, M., Carrier, D., Smith, I. C. P., and Jarrell, H. C., 1990, *J. Am. chem. Soc.*, **112,** 1373.
[19] Mannock, D. A., Lewis, R. N. A. H., and McElhaney, R. N., 1990, *Biochemistry*, **29,** 7790.
[20] Sen, A., Hui, S.-W., Mannock, D., Lewis, R. N. A. H., and McElhaney, R. N., 1990, *Biochemistry*, **29,** 7799.
[21] Lewis, R. N. A. H., Mannock, D. A., and McElhaney, R. N., 1990, *Zentralbl. Bakteriol., Suppl.*, **20,** 643.
[22] Lis, L. J., Tamura-Lis, W., Lim, T., and Quinn, P. J., 1990, *Biochim. Biophys. Acta*, **1021,** 201.
[23] Hinz, H.-J., Kuttenreich, H., Meyer, R., Renner, M., Freund, R., Koynova, R., Boyanov, A., and Tenchov, B., 1991, *Biochemistry*, **30,** 5125.
[24] Chupin, V., Morosova, N., Serebrennikova, G., and Evstigneeva, R., 1991, *Biol. Membr.*, **8,** 638.
[25] Mannock, D. A., and McElhaney, R. N., 1991, *Biochem. Cell Biol.*, **69,** 863–868.
[26] Mannock, D. A., Lewis, R. N. A. H., McElhaney, R. N., Akiyama, M., Yamada, H., Turner, D. C., and Gruner, S. M., 1992, *Biophys. J.*, **63,** 1355.
[27] Turner, D., Wang, Z.-G., Gruner, S. M., Mannock, D., and McElhaney, R. N., 1992, *J. Phys. II France*, **2,** 2039.
[28] Kuttenreich, H., Hinz, H.-J., Koynova, R., and Tenchov, B., 1993, *Chem. Phys. Lipids*, **66,** 55.

[29] KOYNOVA, R., TENCHOV, B., KUTTENREICH, H., and HINZ, H.-J., 1993, *Biochemistry*, **32,** 12437.
[30] MANNOCK, D. A., MCELHANEY, R. N., HARPER, P. E., and GRUNER, S. M., 1994, *Biophys. J.*, **66,** 734.
[31] CUNNINGHAM, B. A., BRAS, W., LIS, L. J., and QUINN, P. J., 1994, *J. Biochem. Biophys. Meth.*, **29,** 87.
[32] BOULIN, C., KEMPF, R., KOCH, M. H. J., and MCLAUGHLIN, S. M., 1986, *Nucl. Instr. Meth. Phys. Res.*, **A249,** 399.
[33] BUNN, C. W., and HOWELL, E. R., 1954, *Nature*, **174,** 549.
[34] TATE, M. W., and GRUNER, S. M., 1989, *Biochemistry*, **28,** 4245.
[35] TATE, M. W., SHYAMSUNDER, E., GRUNER, S. M., and D'AMICO, K. L., 1992, *Biochemistry*, **31,** 1081.
[36] TENCHOV, B. G., 1991, *Chem. Phys. Lipids*, **57,** 165.
[37] *International Tables for Crystallography*, 1983, Vol. A, edited by T. Hahn (Dordrecht: D. Riedel).
[38] SEDDON, J. M., 1990, *Biochim. Biophys. Acta*, **1031,** 1.
[39] SEDDON, J. M., HOGAN, J. L., WARRENDER, N., and PEBAY-PEYROULA, E., 1990, *Prog. Colloid Polymer Sci.*, **81,** 189.
[40] RUOCCO, M. J., ATKINSON, D., SMALL, D. M., SKARJUNE, R. P., OLDFIELD, E., and SHIPLEY, G. G., 1981, *Biochemistry*, **20,** 5957.
[41] REED, R. A., and SHIPLEY, G. G., 1987, *Biochim, Biophys. Acta*, **896,** 153.
[42] MARSH, D., and SEDDON, J. M., 1982, *Biochim. Biophys. Acta*, **690,** 117.
[43] KOYNOVA, R. D., TENCHOV, B. G., QUINN, P. J., and LAGGNER, P., 1988, *Chem. Phys. Lipids*, **48,** 205.
[44] SEDDON, J. M., CEVC, G., KAYE, R. D., and MARSH, D., 1984, *Biochemistry*, **23,** 2634.
[45] GRUNER, S. M., TATE, M. W., KIRK, G. L., SO, P. T. O., TURNER, D. C., KEANE, D. T., TILCOCK, C. P. S., and CULLIS, P. R., 1988, *Biochemistry*, **27,** 2853.
[46] LINDBLOM, G., and RILFORS, L., 1989, *Biochim. Biophys. Acta*, **988,** 221.
[47] BRIGGS, J., and CAFFREY, M., 1994, *Biophys. J.*, **66,** 573.
[48] GRUNER, S. M., 1985, *Proc. Natl. Acad. Sci. USA*, **82,** 3665.
[49] SHYAMSUNDER, E., GRUNER, S. M., TATE, M. W., TURNER, D. C., SO, P. T. O., and TILCOCK, C. P. S., 1988, *Biochemistry*, **27,** 2332.
[50] SIEGEL, D., and BANSCHBACH, J., 1990, *Biochemistry*, **29,** 5975.
[51] ERBES, J., CZESLIK, C., HAHN, W., WINTER, R., RAPPOLT, M., and RAPP, G., 1994, *Ber. Bunsenges. Phys. Chem.*, **98,** 1287.
[52] SEDDON, J. M., CEVC, G., and MARSH, D., 1983, *Biochemistry*, **22,** 1280.